Keeping it Cool in Gas Turbines

By A.V. Rubekina, A.V. Ivanov, G.E. Dumnov, A.A. Sobachkin (Mentor Graphics Corp., Russia); K.V. Otryahina (PAO NPO Saturn, Russia).

One of the key problems in the design of advanced gas turbine engines is the development of effective cooling methods for the turbine vanes and blades. Due to competition and continuous improvement an increased complexity of cooling technology is required in the design of turbine engine parts. In view of the material and time costs for experimental research, CFD has been accepted by turbomachinery companies as one of the main methods for evaluating the performance of new designs. Industrial CFD applications range from classical single- and multi blade-row simulations in steady and transient mode to heat transfer and combustion chamber simulations.

Depending on the type of machine, physical and geometrical effects have to be taken into account. A complicating factor is that it is necessary to carry out parametric studies considering several geometric options in the process of designing the cooling systems. This normally takes a lot of time to generate mesh models due to the mesh resolution required in the boundary layer. With this in mind, PAO NPO Saturn investigated FloEFD's accuracy for this application with the goal of taking advantage of its CAD embedded technology and automatic meshing to significantly reduce the overall simulation time and allow them to frontload their design process. The investigation looked at three different cases.

The first case is the NASA C3X Vane Experiment. This case consists of a 2D blade cascade consisting of three vanes characteristic of a first-stage turbine. Geometry parameters of vane and cooling channels were taken from Hylton et al (1983). Each of the vanes was cooled by an array of ten radial cooling holes. The vanes were fabricated of stainless steel, which has a relatively low thermal conductivity.

The cooling parameters such as average temperature and mass flow rate are presented in Table 1.

Three mesh configurations were analyzed. For coarse mesh M1 number of cells was about 25.500, for medium mesh M2~48.000, for fine mesh M4~121.400 cells. These meshes had the same topology, but basic mesh density was varied. Around the central vane all cells were additionally refined by two levels and into cooled channels by three levels.

The calculation results for each mesh are presented in Figure 2. Figures 3-4 show temperature and heat transfer coefficient distributions along surface of vane. Negative distances indicate the probe positions on the pressure side. Positive values indicate the suction side locations of temperature measurements. The peak in heat transfer coefficient distribution is observed on the suction side of the vane. This is due to the more rapid laminar-turbulent transition in boundary layer as compared to experiment where this transition was also observed but was smoother.

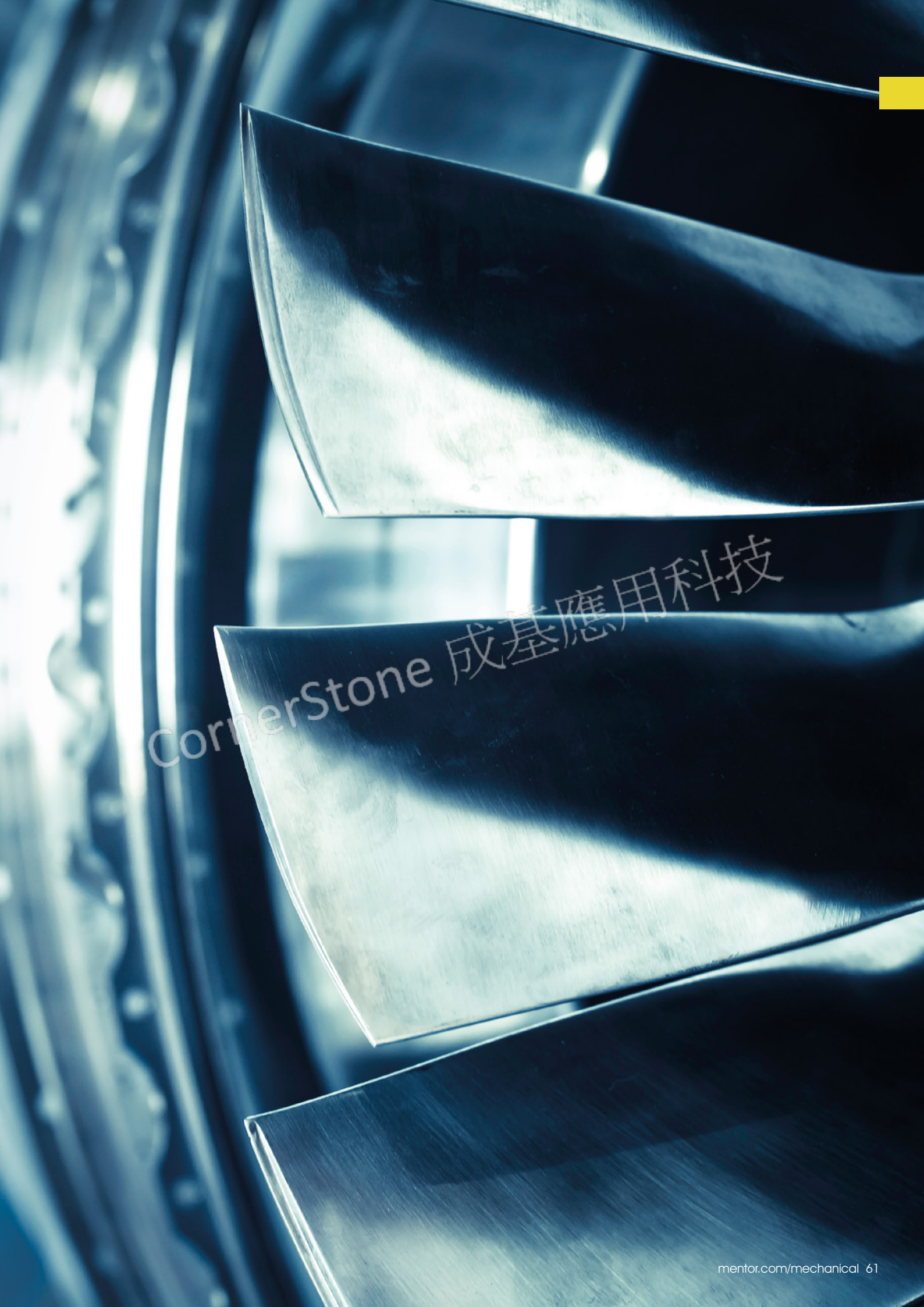

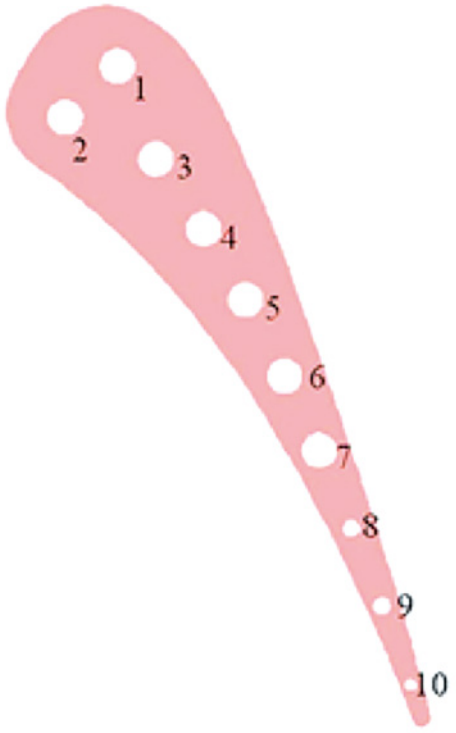

Figure 1. Vane section with ten cooling channels

Channel number	1	2	3	4	5	6	7	8	9	10
D, mm	6.3	6.3	6.3	6.3	6.3	6.3	6.3	3.1	3.1	3.1
G, g/sec	7.79	6.58	6.34	6.66	6.52	6.72	6.33	2.26	1.38	0.68
T, K	371	375	360	364	344.5	399	359	358	418	450

Table 1. Parameters of cooled channels

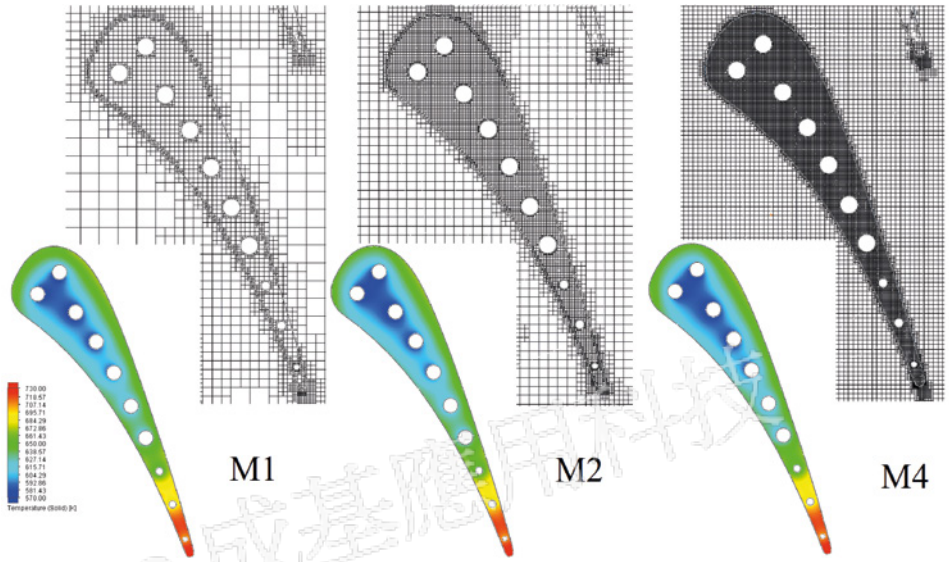

Figure 2. Temperature distribution computed for each mesh configuration

Maximum and average values of calculation discrepancies are showed in Table 2. The results obtained even for the coarse mesh have a good agreement with experimental data.

The second study consisted of a showerhead film cooled vane, five rows of staggered cylindrical cooling holes is used in Nasir et al (2008). The vane cascade consists of four full vanes and two partial vanes. The number of cooling holes on the stagnation region row is 17. Cooling flow is injected at 90° angle to the freestream and 45° angle to the span of the vane. Overview and dimensions of the test vane is presented in Figure 5.

The computational mesh with about 133,000 cells was used.

Figure 6 shows the local Mach number distributions on the vane without film cooling holes. It is plotted against non-dimensional surface distance s/C. The Mach number distribution varies smoothly along the pressure side. The flow on the suction side continuously accelerates up to the throat area (s/C = 0.51).

Figure 7 shows the distribution of the gas temperature (left) and cooling air streamlines with the Mach number distribution on the air-gas channel (right).

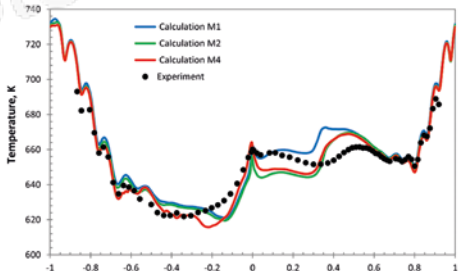

Figure 3. Comparison of calculations with measurements for temperature distribution

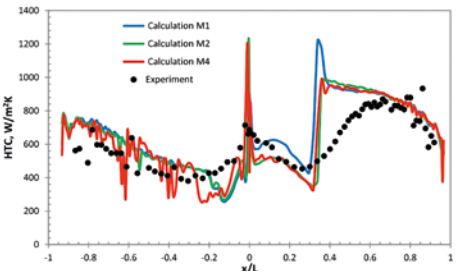

Figure 4. Comparison of calculations with measurements for heat transfer coefficient distribution

	Mesh (M1)		Mesh (M2)		Mesh (M4)	
	Suction Side	Pressure Side	Suction Side	Pressure Side	Suction Side	Pressure Side
Max. error, %	7.79	6.58	6.34	6.66	6.52	6.72
Aver. error, %	371	375	360	364	344.5	399

Table 2. Surface temperature calculation discrepancies

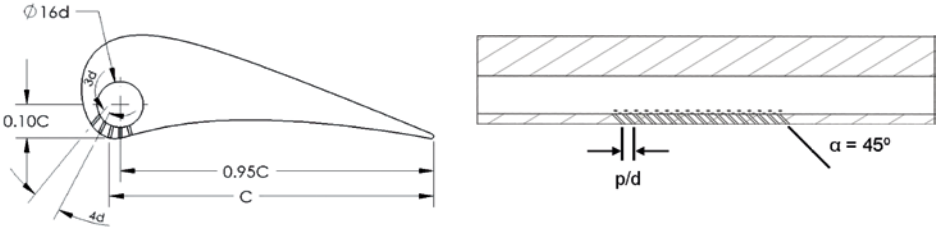

Figure 5. Profile view of showerhead film cooled vane (left) and section view of stagnation row of holes (right)

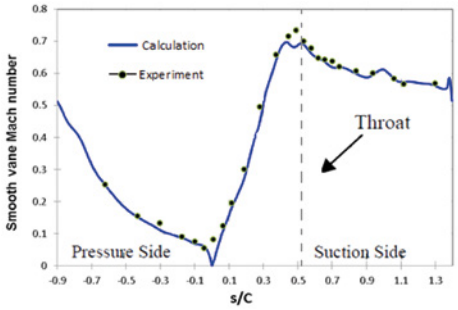

Figure 6. Comparison of computed and measured smooth vane Mach number

The final case is a rotor blade used by NPO Saturn. The detailed description of similar blade can be found in Vinogradov et al (2016). General view of the blade and the internal channels are shown in Figure 8. The blade is made of heat-resistant alloy ZS32. Ceramic coating (a thickness of 0.02-0.03 mm with thermal conductivity λ=2-3 W/(m·K)) serves to insulate components from large and prolonged heat loads by utilizing thermally insulating materials.

Relatively cold air is passed through the passages inside the turbine blade. Complicated internal cooling system includes serpentary channels with rib turbulators. Then coolant goes out the blade through holes located on the blade tip. The remaining coolant is ejected from the trailing edge of the profile.

As for previous test cases evaluation of the temperature distribution of the blade was made by means of conjugate heat transfer simulation. Ceramic heat barrier coating was taken account as the thermal resistance with equivalent parameters. Numerical simulation included modeling of mainstream gas flow, air flow through the internal channels of the blade as well as heat transfer in solid and between fluid and solid by convection. The computational mesh with about 944 000 cells was used.

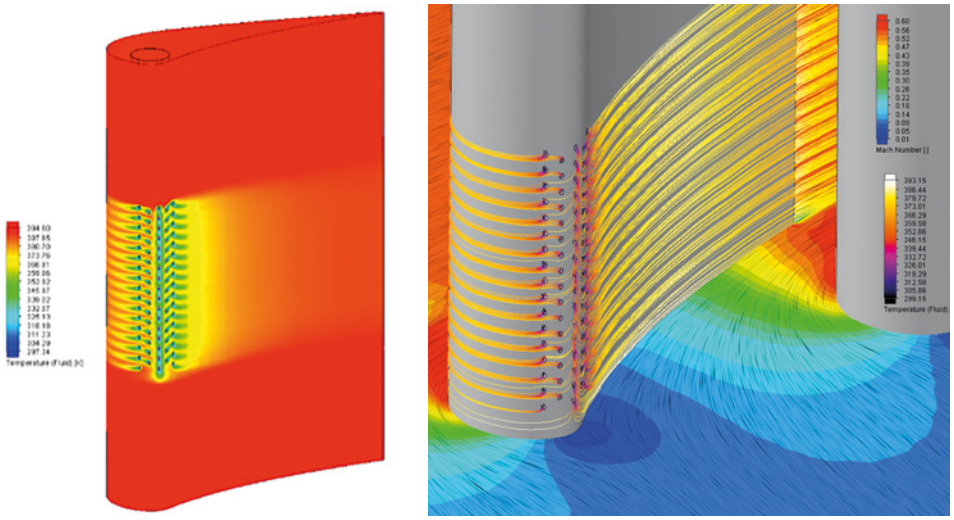

Figure 7. Gas temperature distribution (left) and cooling air streamlines with the Mach number distribution (right)

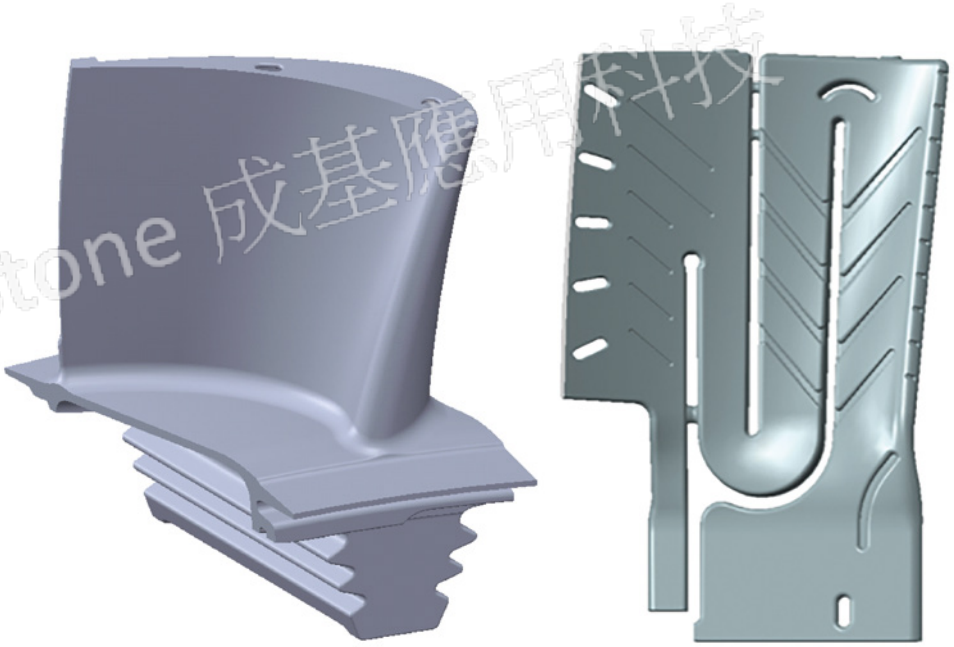

Figure 8. CAD model of simulated blade (left) and its internal passages (right)

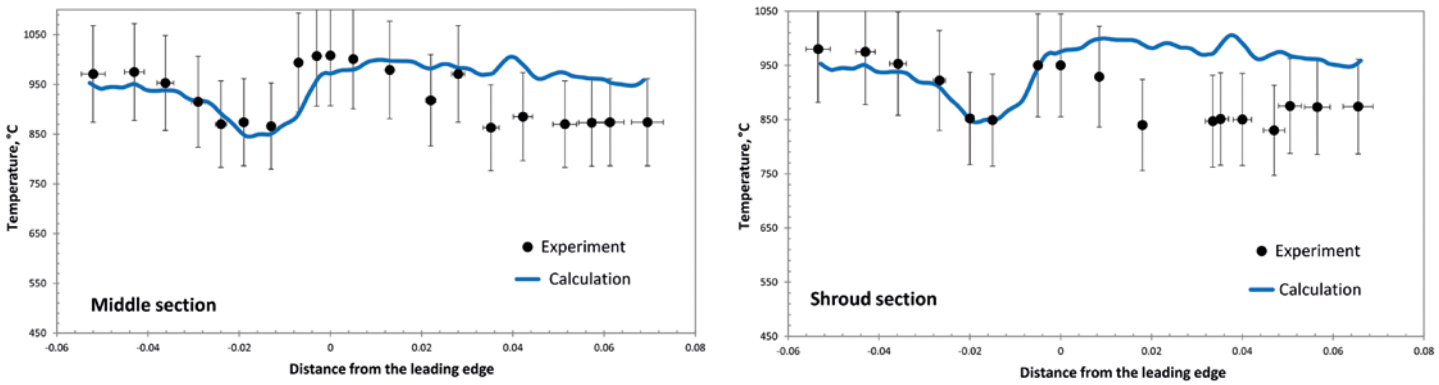

Figure 9. Comparison of computed and measured surface temperature along the profile in shroud section and middle section of the blade

Shroud and middle sections of the blade were taken for comparison of numerical simulations with experimental data (see Figure 9). Marked on the Figure range of ratio error is 10%. One can see that difference between computations and experimental data is within this ratio for pressure side of the blade both for shroud and middle section. For suction side of the blade agreement with the experimental data is a bit worse particularly in shroud section. Calculation discrepancies are estimated at the level of 15% there.

Shown in Figures 10 and 11 pressure and cooling air temperature distributions along flow streamlines as well as surface metal temperature field on both side of the blade are in a good concordance with qualitative evaluates.

Calculated gas mass flow rate through blade row is equal to 29.94 kg/sec. Mass flow rate through one blade is equal to 0.027 kg/sec. Caused by heat exchange with hot metal blade coolant air temperature increment is about 110°C. Obtained results are also in a good agreement with qualitative estimations.

Obtained computation results for these test models are in a good agreement with experimental data. The predicted blade temperature distribution and flow through the blade for industrial convective cooled turbine blade are also in a good agreement with available experimental data in the qualitative and quantitative aspects.

It shows that with FloEFD users can achieve acceptable accuracy on far coarser meshes when compared with traditional CFD approaches. Therefore computations of fluid flow and heat transfer for even complex 3D cases take relatively modest computational resources making FloEFD a useful CFD tool for engineering numerical simulation of heat transfer in vanes and blades.

This article is a summary of the paper: Using Modern CAD-Embedded CFD Code for Numerical Simulation of Heat Transfer in Vanes and Blades. A.V. Rubekina, A.V. Ivanov, G.E. Dumnov, A.A. Sobachkin, Mentor Graphics Corp., Russia; and K.V. Otryahina, PAO NPO Saturn, Russia

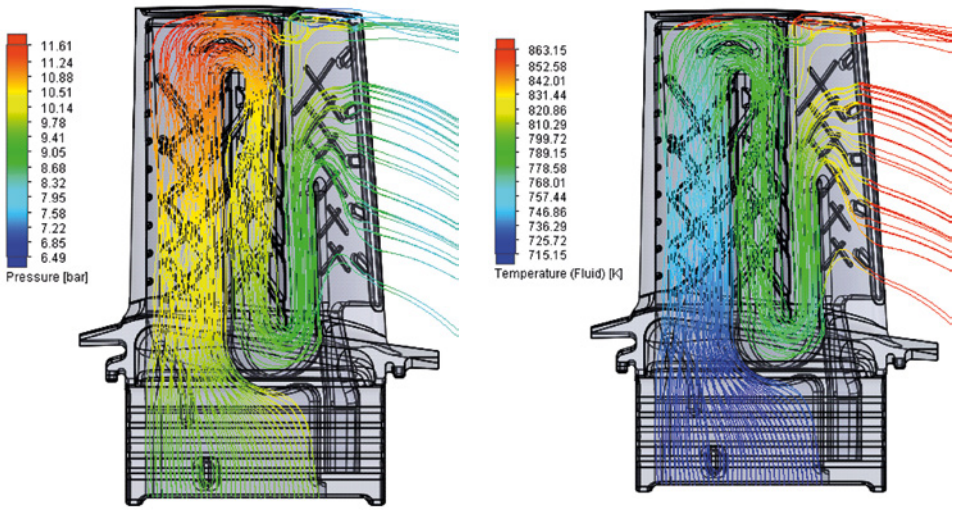

Figure 10. Flow streamlines colored by pressure (left) and the cooling air temperature (right) into passages

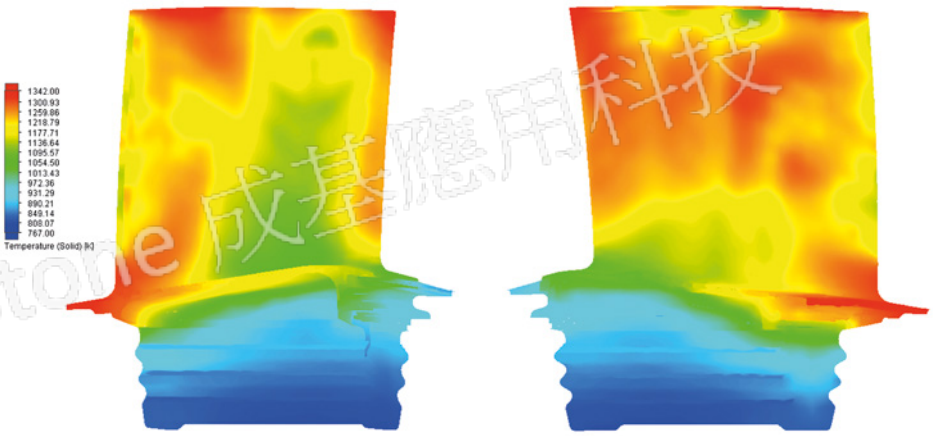

Figure 11. Distribution of solid temperature on the pressure side (left) and on the suction side (right)

References

[1] Hylton, L.D., Mihelc, M.S., Turner, E.R., Nealy, D.A., and York, R.E. (1983) 'Analytical and Experimental Evaluation of the Heat Transfer Distribution Over the Surface of Turbine Vanes', NASA Paper No. CR-168015.

[2] Nasir, S., Bolchoz, T., Ng, W.F., Zhang, L.J., Moon, H.K., Anthony, R.J. (2008) 'Showerhead Film Cooling Performance of a Turbine Vane at High Freestream Turbulence in a Transonic Cascade', ASME IM-ECE-2008-66528, 2008.

[3] Sobachkin, A.A., Dumnov, G.E. (2013) 'Numerical Basis of CAD-Embedded CFD', Proceedings of NAFEMS World Congress NWC 2013, Austria, Salzburg, June 09-12, 2013.

[4] Vinogradov, K.A., Kretinin, G.V., Otryahina, K.V., Didenko, R.A., Karelin, D.V., Shmotin, Y.N. (2016) 'Robust optimization of the HPT blade cooling and aerodynamic efficiency', ASME GT2016-56195, 2016.